Hindawi
International Journal of Polymer Science
Volume 2018, Article ID 1782734, 8 pages
https://doi.org/10.1155/2018/1782734

*Research Article*

# Identification of a Novel Anticancer Oligopeptide from *Perilla frutescens* (L.) Britt. and Its Enhanced Anticancer Effect by Targeted Nanoparticles *In Vitro*

**Dong-Liang He,[1,2] Ri-Ya Jin,[1] Hui-Zhen Li,[1] Qing-Ye Liu,[1] and Zhi-Jun Zhang[1]**

[1]*School of Chemical Engineering and Technology, North University of China, Taiyuan, China*
[2]*Department of Environmental Engineering, Taiyuan Institute of Technology, Taiyuan, China*

Correspondence should be addressed to Zhi-Jun Zhang; zjzhang@nuc.edu.cn

Received 14 April 2018; Revised 15 June 2018; Accepted 26 June 2018; Published 9 August 2018

Academic Editor: Jianxun Ding



*Objective*. *Perilla frutescens* (L.) Brittis is a dietary herbal medicine and has anticancer effect. However, little is known about its anticancer peptides. This study is aimed at identifying cytotoxic oligopeptides which are loaded by a drug delivery system, to explore its anticancer application. *Methods*. The oligopeptides were isolated from enzymatic hydrolysates of *Perilla* seed crude protein by using ultrafiltration, gel filtration chromatography, and reversed-phase high-performance liquid chromatography (RP-HPLC). The structure of the oligopeptide was determined using a peptide sequencer, and its anticancer effect was examined by the MTT assay. PSO (*Perilla* seed oligopeptide), the most potent anticancer oligopeptide, was loaded by chitosan nanoparticles (NPs) modified by hyaluronic acid (HA). Then, the particle size, zeta potential, encapsulation efficiency (EE), drug loading efficiency (LE), the cumulative release rates of NPs, and its cytotoxic effect on cancer cells were investigated. *Results*. Three fractions were isolated by the chromatography assay. The third fraction has a broad-spectrum and the strongest anticancer effect. This fraction was further purified and identified as SGPVGLW with a molecular weight of 715 Da and named as PSO. Then, PSO was loaded by HA-conjugated chitosan to prepare HA/PSO/C NPs, which had a uniform size of 216.7 nm, a zeta potential of 35.4 mV, an EE of 38.7%, and an LE of 24.3%. HA/PSO/C NPs had a slow release rate *in vitro*, with cumulative release reaching to 81.1%. Compared with free PSO, HA/PSO/C NPs showed notably enhanced cytotoxicity and had the strongest potency to human glioma cell line U251. *Conclusion*. This study demonstrated that PSO, a novel oligopeptide from *Perilla* seeds, has a broad-spectrum anticancer effect and could be encapsulated by NPs, which enhanced tumor targeting cytotoxicity with obvious controlled release. Our study indicates that *Perilla* seeds are valuable for anticancer peptide development.

## 1. Introduction

*Perilla frutescens* (L.) Britt. has a long cultivation history of more than two thousand years [1] and has been identified as a medicine-food homology plant by the Ministry of Health, China [2]. The seed of *Perilla frutescens* has been regarded as one of the major officinal parts and has special anticancer effects [3], has neuroprotective ability [4], boosts memory [5, 6], improves eyesight [7], lowers blood lipid and blood pressure [8], and inhibits platelet aggregation. Proteins comprise 20%~23% of the total mass of *Perilla frutescens* seeds and can be up to 28%~45% after being defatted. However, the *Perilla frutescens* seed is only a kind of vegetable healthcare oil, and the by-product after oil extraction has not acquired wide attention. Extensive research on protein resource of *Perilla frutescens* seeds is necessary for the purpose of efficient use.

Safe and effective anticancer drugs have always been the important directions in the drug research and development field. Oligopeptides, as short-chain polypeptides, have been considered promising candidates due to potent activity, higher safety, and absorbability. They can induce apoptosis of cancer cells, destroy membranaceous cell and organelle structures, change the pH level inside the cell and tumor microenvironment, and enhance immune responses to tumor by the body. And oligopeptides present low toxicity

or nontoxicity to normal cells. Thus, an oligopeptide has emerged as one of the hot topics in the anticancer drug field. Several oligopeptides have been carried out on clinical stage against tumor, such as tyroserleutide [9] and tyroservatide [10, 11]. Plitidepsin (Aplidin®), a cyclic depsipeptide, has been evaluated in a phase III clinical trial for multiple myeloma [12]. Tasidotin (ILX651), a depsipeptide from sea slug, has reached a phase II clinical trial for advanced or metastatic non-small-cell lung cancer [13]. These oligopeptides are nature products isolated from the body of animals and plants, and so far, they can yield better anticancer effect after synthesis and ingeniously structural modification. Therefore, screening anticancer oligopeptides from *Perilla frutescens* might be meaningful for the development of *Perilla* protein.

Oligopeptide utilization is limited by their nature, such as instability, short half-life, and easy degradation in plasma; however, these deficiencies could be overcome by using macromolecular peptide delivery systems and tumor-targeting agents [14]. Chitosan is a natural cationic polymer and can be used as a drug delivery system due to its good biodegradability and biocompatibility [15]. Hyaluronic acid (HA) binds to its receptor (CD44) to participate in the regulation of tumor growth and metastasis. Based on this feature, initiative targeting effect on tumor can be acquired by using the binding activity between HA and CD44 [16, 17]. It has been reported that HA-conjugated chitosan nanoparticles (NPs) can be effectively utilized as an active tumor-targeting drug carrier.

In this study, oligopeptides were isolated and purified from *Perilla* meal protein, and their anticancer effects were screened. Then, the most potent antitumor oligopeptide was encapsulated by NPs using HA-conjugated chitosan, and its targeting cytotoxicity to several tumor cells was evaluated.

## 2. Materials and Methods

*2.1. Preparation of Defatted Flour and Crude Protein.* After drying at 37°C for 2 h, *Perilla* seeds were milled and passed through a 60-mesh-size sieve. The sieved flour was defatted by using 3 times volume of petroleum ether with stirring for 30 min in an extractor. After repeating for 3 times and drying at 50°C for 1 h, the defatted flour was obtained.

The flour was suspended in water with a biomass-to-volume ratio of 1 : 10, with pH adjusted to 10 by adding sodium hydroxide. After incubation for 60 min at 55°C, the alkali-aided solubilized proteins were collected in supernatant by centrifugation. Isoelectric protein precipitation was applied by the addition of hydrochloric acid (HCl), followed by centrifugation at 10,000 rpm at 4°C for 20 min.

*2.2. Protein Hydrolysis, Ultrafiltration, and Isolation. Perilla* crude protein was dissolved into water (30 mg/ml); then, alcalase (more than $1.9 \times 10^4$ U/g) was added (Novozymes, Denmark). After incubation for 6 hours at 60°C and pH 9.5, the enzyme in the hydrolysate was inactivated at 100°C, followed by cooling to 37°C and then centrifuging to collect the supernatant. Hydrolysate fractions with molecular weight smaller than 3 kDa were obtained through centrifugation with an ultrafiltration tube with 3 kDa cut-off (Millipore, Temecula, CA, USA). Oligopeptide fractions below 3 kDa were further purified by Sephadex G-25 (1.6 cm × 100 cm) preequilibrated with distilled water. Oligopeptides were eluted with distilled water at 0.5 ml/min and collected one tube per 4 min. Aliquots were monitored by measuring the absorbance at 214 nm and pooled within the same peak area. The cytotoxic activity of lyophilized fractions was evaluated by the MTT assay.

*2.3. Oligopeptide Purification by Reversed-Phase High-Performance Liquid Chromatography (RP-HPLC).* Oligopeptide was dissolved in water (0.5 mg/ml) and then was purified by RP-HPLC with the C18 column (4.6 × 250 mm, 5 $\mu$m, Agilent, USA). The conditions were as follows: a linear gradient of acetonitrile containing 0.1% TFA increasing from 5% to 40% over 60 min and a flow rate of 1.0 ml/min. The fractions were collected, lyophilized, and named PSO (*Perilla* seed oligopeptide).

*2.4. Molecular Mass and Sequence Analysis.* The amino acid sequence was determined by the Edman degradation method using a protein sequencer (PPSQ-23A, Shimadzu, Japan). And the molecular mass was analyzed by Agilent 6210 time-of-flight LC/MS (Agilent Technologies, Santa Clara, CA).

*2.5. Preparation of PSO-Loaded NPs.* Purified PSO was dissolved in water (1.0 mg/ml); then, the same volume of 2.5 mg/ml chitosan aqueous solution in 0.1 mol/l acetic acid (pH 4.0) was added. After stirring for 10 min, tripolyphosphate was added (0.15 mg/ml). After continuous stirring for 30 min, precipitation was collected by centrifugation at 14,000 rpm for 30 min, and then PSO-loaded chitosan was obtained by lyophilization.

1-Ethyl-3-(3-dimethylaminopropyl)carbodiimide (EDC) was added to 3 mg/ml HA aqueous solution. After EDC was dissolved completely, N-hydroxysuccinimide was added; then, the pH was adjusted to 7.5. After incubation at 37°C for 3 hours, lyophilized powder of PSO-loaded chitosan was suspended in HA solution with a biomass ratio of 4 : 1. After stirring for 24 hours, the mixture was centrifuged at 14,000 rpm at 4°C for 60 min; then, PSO-loaded HA-conjugated chitosan (HA/PSO/C) NPs were obtained by lyophilization.

*2.6. Characterization of HA/PSO/C NPs.* HA/PSO/C NPs were suspended in water (30 mg/ml) and then were ultrasonicated for 5 min. A particle analyzer (Zetasizer Nano ZS90, Malvern Instruments Ltd., United Kingdom) was used to assay the mean particle size and zeta potential of HA/PSO/C NPs. All measurements were performed in triplicate.

*2.7. Encapsulation Efficiency (EE) and Drug Loading Efficiency (LE) of HA/PSO/C NPs.* 1 mg of HA/PSO/C NPs was degraded by 10% HCl and then diluted with ethanol to 10 ml. PSO concentration was assayed by high-performance liquid chromatography (HPLC). EE was defined as the percentage of the mass of the loaded PSO to the total mass of the consumed PSO in HA/PSO/C NPs preparation, and

LE was defined as the percentage of loaded-PSO mass to NPs mass.

*2.8. In Vitro Drug Release Profiles.* 1.5 mg of HA/PSO/C NPs was suspended in phosphate-buffered saline (PBS, pH 7.4) (0.5 mg/ml) and then was transferred into a dialysis membrane bag (2000 of molecular weight cut-off, Sangon, Shanghai, China) which was soaked in 30 ml PBS. The whole dialysis system was shaken at 37°C in an incubator. At different time intervals, 1 ml of released solution was collected for HPLC analysis, and the equivalent volume of fresh PBS was compensated. The cumulative release of PSO was measured in triplicate.

*2.9. Cell Culture and Reagents.* Cell lines of human glioma (U251), human lung carcinoma (A549), human colorectal carcinoma (HCT116), human gastric carcinoma (MGC-803), and human hepatocellular carcinoma (HepG2) were purchased from the Chinese Academy of Sciences (Shanghai, China) and were maintained in DMEM containing 10% fetal bovine serum at 37°C in a humidified incubator supplemented with 5% $CO_2$.

*2.10. Measurement of Inhibition on Cell Proliferation through the MTT Method.* The cancer cells in the logarithmic phase were trypsinized to single-cell suspension, and a 96-well plate was seeded with $0.2 \times 10^5$ cells per well. After overnight incubation, medium containing the indicated sample was added in a total volume of 100 $\mu$l. After the designated time point, 10 $\mu$l of the MTT reagent was added into corresponding wells of the plate, and the optical density (OD) at a wavelength of 450 nm was detected with a microplate reader. Proliferation rates were defined as the percentage of the corresponding sample OD to the vehicle control OD, which was set at 100%. Dose-response curves and the concentration inhibiting proliferation by 50% (IC50) were generated with GraphPad Prism 4.0 (GraphPad Software, La Jolla, CA).

*2.11. Statistical Processing.* Data were presented as mean ± standard deviation (SD) and processed with Statistical Product and Service Solutions 19.0 (SPSS 19.0). Statistical analysis was performed via one-way analysis of variance. $P < 0.05$ suggested that the difference had statistical significance.

## 3. Results and Discussions

Anticancer peptides, which can directly kill cancer cells with little damage to normal human cells, are new kinds of anticancer drugs and have become a hot spot in new anticancer drug research [18]. Hundreds of anticancer peptides have been found so far [19]. And appropriate structural modifications lead to more potent efficacy of anticancer peptides. In the present study, a novel anticancer oligopeptide was isolated from *Perilla frutescens* seeds. And the anticancer effect was enhanced by form modification through HA-conjugated chitosan.

Oligopeptides smaller than 3 kDa were separated by ultrafiltration from alcalase hydrolysate of *Perilla* crude protein. After isolation by Sephadex G-25, oligopeptide fractions were separated into three major fraction peaks (Figure 1(a)), named as $PSO_{(G25)}1$, $PSO_{(G25)}2$, and $PSO_{(G25)}3$. After pooling and lyophilization, the cytotoxicity of these eluted products was examined by the MTT assay (Figure 1(b)). Compared with $PSO_{(G25)}1$ and $PSO_{(G25)}2$, $PSO_{(G25)}3$ showed the strongest anticancer effect by evaluating the trend presenting the lowest proliferative activity on several cancer cells (U251, A549, HCT116, and HepG2) at both dosages of 1 mg/ml and 5 mg/ml, and the inhibitive effect was in a dose-dependent manner in that 5 mg/ml showed significant inhibition than 1 mg/ml ($P < 0.05$). Although $PSO_{(G25)}3$ did not show the strongest anticancer effect on MGC-803, 5 mg/ml $PSO_{(G25)}3$ still led to a significant decrease in proliferation compared to the vehicle group ($P < 0.001$). This result indicated that $PSO_{(G25)}3$, as a novel anticancer oligopeptide, possessed a broad spectrum of anticancer activities. $PSO_{(G25)}3$ showed a mild cytotoxicity to HepG2 (hepatocellular carcinoma cell line) and MGC-803 (gastric carcinoma cell line) and a moderate cytotoxicity to HCT116 (colorectal carcinoma cell line) and A549 (lung carcinoma cell line). Remarkably, $PSO_{(G25)}3$ possessed the strongest antiproliferative activity to U251 (glioma cell line), which might be correlated to its neurological function. It has been recorded that *Perilla frutescens* seeds were used as the main ingredient to treat neurological diseases, such as anxiety, in the prescription from Chinese ancient works "Yan Shi Ji Sheng Fang." In addition, $PSO_{(G25)}1$ showed relative higher inhibitive effect against MGC-803, compared to $PSO_{(G25)}2$ and $PSO_{(G25)}3$, which indicated the gastric carcinoma preference of $PSO_{(G25)}1$. Taken together, we focused our further study on $PSO_{(G25)}3$ for structural analysis, modification, and its anticancer efficacy.

Then, lyophilized $PSO_{(G25)}3$ was purified by RP-HPLC and determined the sequence of Ser-Gly-Pro-Val-Gly-Leu-Trp, which was named as PSO. PSO molecular mass was practically measured as 715.33 Da (Figure 2), which was anastomosed essentially with theoretical calculated molecular mass (715 Da).

Anticancer peptides are increasingly getting attention; however, deficiencies still exist, such as low natural production, short half-life [20], and less potent bioactivity in plasma [21], as well as easy degradation [19]. Enhancing the stability and tumor-targeting effects of anticancer peptides will definitely improve their antitumor effects. Chitosan nanoparticle carriers have distinct advantages of water solubility, electropositivity, low toxicity, biodegradability, biocompatibility, mass production, and controlled release [22]. In this study, we aimed to use chitosan as a drug delivery system to encapsulate PSO and hope to extend its release, stability, and half-life. HA is an important constituent of the extracellular matrix and is characterized as a natural and linear mucopolysaccharide with electronegativity, biodegradation, and biocompatibility. Research indicates that HA-specific receptors include CD44, RHAMM, LYVE-1, and HARE [23, 24]. CD44 are highly expressed on the surface of various cancer cells, such as glioma [25], ovarian cancer [26], and lung adenocarcinoma [27]. This characteristic can be applied to the formulation development of pharmaceutical agents for greatly increasing the drug concentration in the target cells [28].

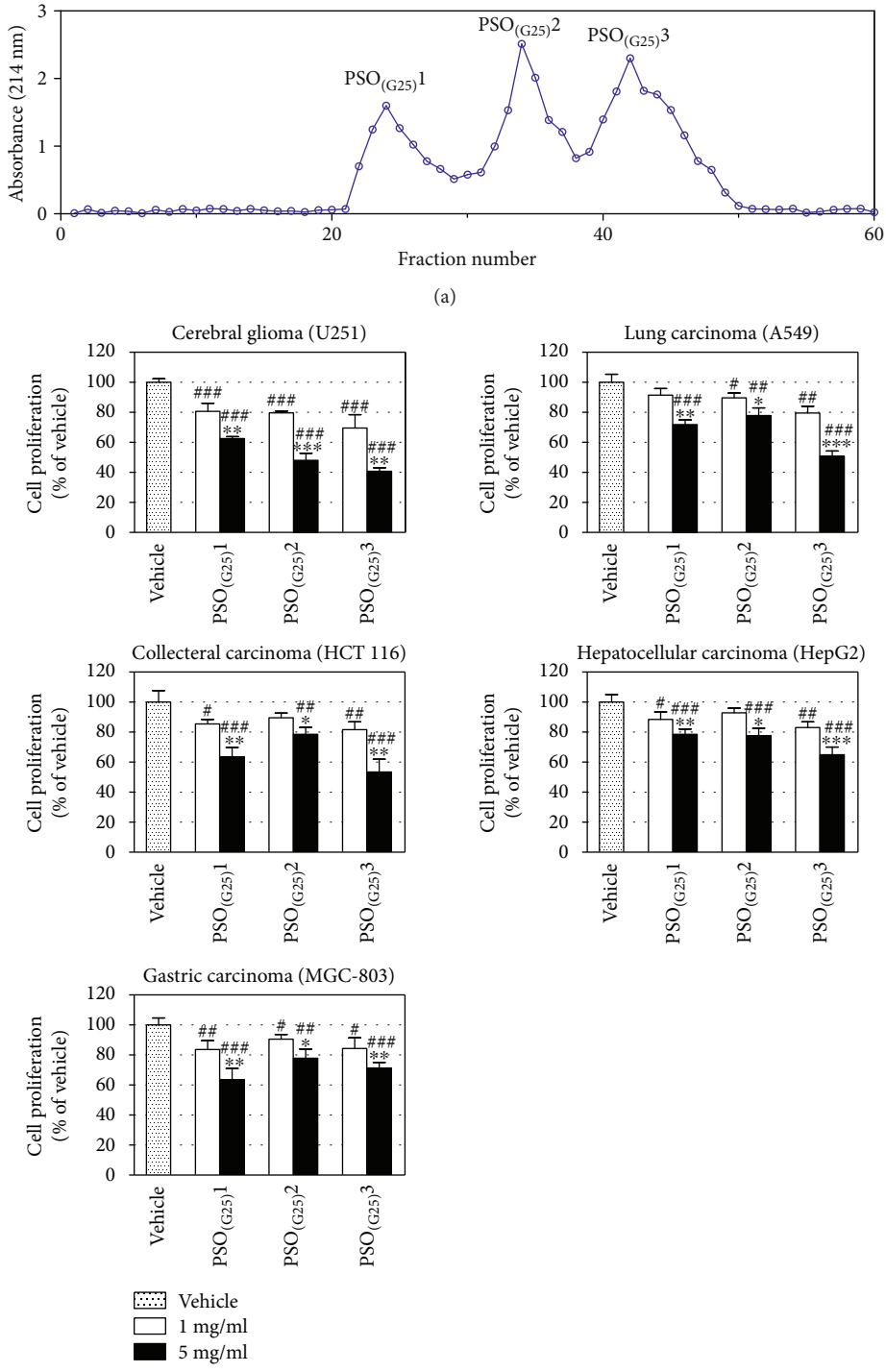


Figure 1: Purification of oligopeptides and their cytotoxicity screening. (a) Gel filtration chromatography on a Sephadex G-25 column, and there were three peaks, $PSO_{(G25)}1$, $PSO_{(G25)}2$, and $PSO_{(G25)}3$. (b) Anticancer effect of three fractions on U251, A549, HCT116, HepG2, and MGC-803 with 1 mg/ml or 5 mg/ml for 24 h, measured by the MTT assay. Percentages of cell proliferation were normalized by optical density values of the vehicle group (as 100%). Data are shown as means ± SD ($n = 5$). $*$ denotes $P < 0.05$, $**$ denotes $P < 0.01$, and $***$ denotes $P < 0.001$; comparisons were performed between groups of 1 mg/ml and 5 mg/ml of every fraction. # denotes $P < 0.05$, ## denotes $P < 0.01$, and ### denotes $P < 0.001$; comparisons were performed against the vehicle group.

In this study, electronegative HA covalently bound to electropositive chitosan via EDC to formulate assembly into NPs with drug loading activity. As shown in Figure 3, HA/PSO/C NPs presented even distribution in particle size with a mean value of 216.7 ± 4.5 nm (Table 1). The sharp main peak suggested that HA/PSO/C NPs had a fairly

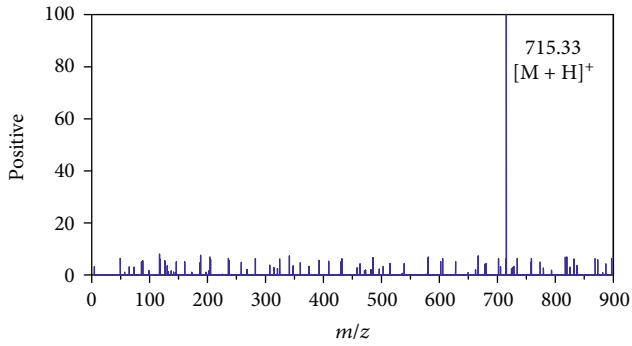


Figure 2: LC/MS analysis of PSO. Consistent with theoretical calculated molecular mass, molecular weight of purified PSO was about 715.33 Da analyzed by Agilent 6210 time-of-flight LC/MS.

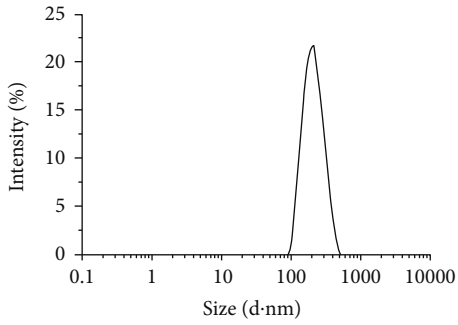


Figure 3: Particle size distribution profiles of HA/PSO/C NPs. Particle size distribution curves of HA/PSO/C NPs measured by a particle analyzer.

Table 1: Characterization of HA/PSO/C NPs (mean ± SD, $n = 3$).

| | Particle size (nm) | Zeta potential (mV) | EE (%) | LE (%) |
|---|---|---|---|---|
| HA/PSO/C | 216.7 ± 4.5 | 35.4 ± 3.2 | 38.7 ± 4.5 | 24.3 ± 1.2 |

narrow size distribution, indicating acceptable size uniformity. The mean zeta potential was 35.4 ± 3.2 mV (Table 1), indicating a satisfactory stability. Moreover, Table 1 also showed EE and LE of HA/PSO/C NPs at 38.7 ± 4.5% and 24.3 ± 1.2%, respectively, indicating successful loading.

The drug release behavior of PSO from HA/PSO/C NPs was also investigated in the release medium of PBS (pH 7.4) at 37°C, according to the ascending velocity of cumulative release curve. As shown in Figure 4, an initial burst release of PSO was noted to 60.7 ± 1.3% within 8 hours. The loaded drug was gradually released from 8 hours to 36 hours, whereas the release velocity became slower. After 36 hours, it hit a release plateau. At the end of the 48-hour release, 81.1 ± 2.3% of PSO was released. The release study indicated that HA/PSO/C NPs had the acceptable abilities of sustained release which could be the contribution from chitosan. Thus, it is speculated that the drug delivery NPs could enhance and prolong the anticancer efficacy of PSO with sustained release

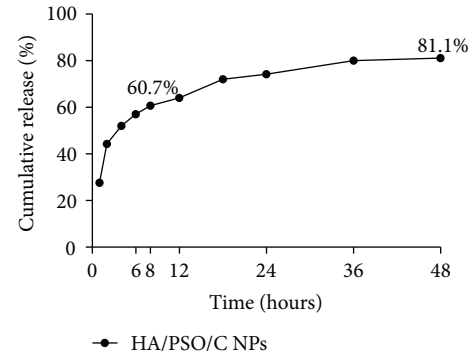


Figure 4: Cumulative release curve. PSO cumulatively released from HA/PSO/C NPs was quantified using HPLC until 48 h. Data are shown as means ± SD ($n = 3$).

into the intracellular tumor microenvironment and reduce systemic cytotoxicity because of the slow release behavior in blood circulation. Taken together, these results of characterization and controlled release suggested that HA/PSO/C NPs were successfully prepared.

Because HA/PSO/C NPs were speculated to be enriched around the tumor and were offered the selection by the contribution from HA due to their binding to specific receptors on the surface of the tumor cell [23, 24], the anticancer effects between HA/PSO/C NPs and PSO were compared to prove it. As shown in Figure 5, 1 mg/ml HA/PSO/C NPs showed inhibitive effect against proliferation of all 5 kinds of cancer cells. Compared with 1 mg/ml PSO, HA/PSO/C NPs showed notably stronger cytotoxic effect on 5 cancer cells ($P < 0.01$) and exhibited the strongest inhibition on U251 (human glioma cell line), then followed by the inhibition on A549 (human lung carcinoma cell line). Furthermore, as shown in Figure 6, HA/PSO/C NPs and PSO could inhibit U251 proliferation with both dose-dependent manner and time-dependent manner. IC50s of HA/PSO/C NPs at 24 hours and 48 hours were 0.39 mg/ml and 0.22 mg/ml, respectively, whereas IC50s of PSO at 24 hours and 48 hours were 2.00 mg/ml and 0.49 mg/ml, respectively. Both IC50s of HA/PSO/C NPs were more potent than IC50s of PSO, which indicated the enhanced potency of PSO by HA-conjugated chitosan NPs. These results suggested that HA/PSO/C NPs worked well for anticancer on various cancer cells. Chitosan and HA worked together to achieve the activity increase. Chitosan, serving as a type of scaffold and macromolecule carrier, has obviously sustained-release property [29]. Drugs can freely diffuse from the chitosan scaffold or even can be released due to the degradation of chitosan [30]. However, the adhesion ability to cells by chitosan is less effective than that by HA. HA affects the adherence and migration ability of tumor cells [31] through binding with specific receptors, such as CD44 [32]. CD44 variants are achieved after splicing and modification and then overexpressed on the surface of tumor cells in abnormal conditions. Overexpressed CD44 variants promote tumorigenicity, migration, and invasion, as well as the binding capability to HA [33]. Therefore, HA, serving as the targeted agent, increases the drug concentration around

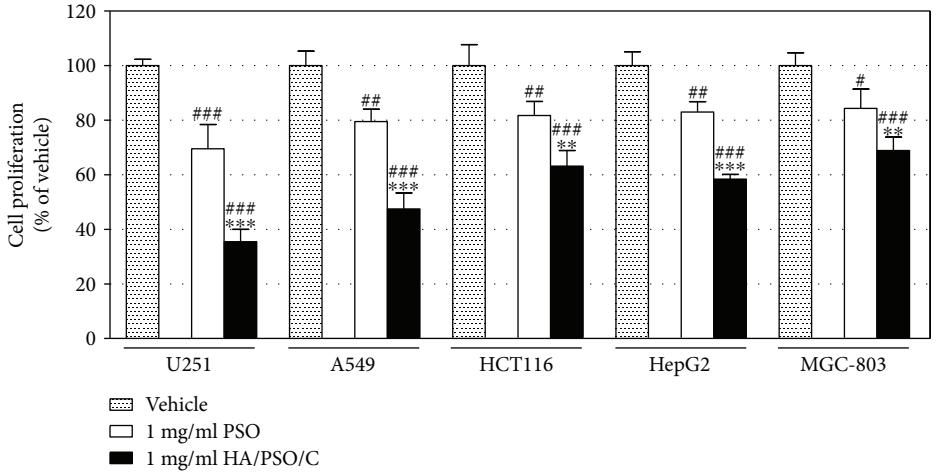


Figure 5: Cytotoxicity of HA/PSO/C NPs on various cancer cells. Anticancer effect of HA/PSO/C NPs or free PSO on U251, A549, HCT116, HepG2, and MGC-803 with 1 mg/ml for 24 h, measured by the MTT assay. Percentages of cell proliferation were normalized by optical density values of the vehicle group (as 100%). Data are shown as means ± SD ($n = 5$). ∗∗ denotes $P < 0.01$, and ∗∗∗ denotes $P < 0.001$; comparisons were performed between groups of HA/PSO/C NPs and PSO. # denotes $P < 0.05$ ## denotes $P < 0.01$, and ### denotes $P < 0.001$; comparisons were performed against the vehicle group.

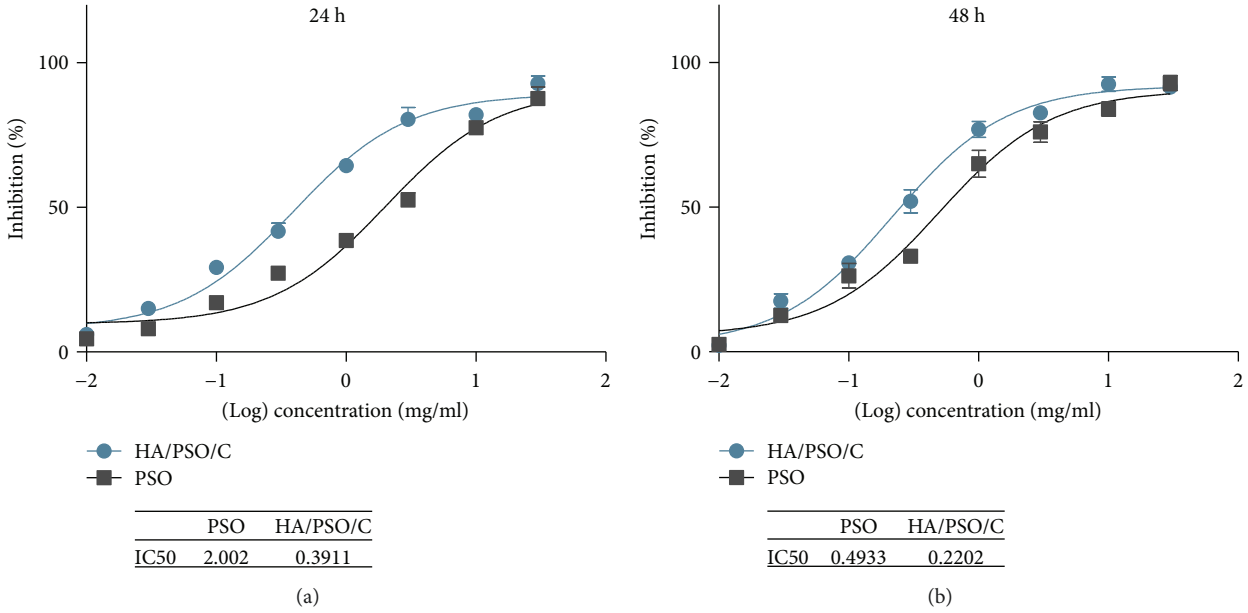


| | PSO | HA/PSO/C |
|---|---|---|
| IC50 | 2.002 | 0.3911 |

(a)

| | PSO | HA/PSO/C |
|---|---|---|
| IC50 | 0.4933 | 0.2202 |

(b)

Figure 6: Enhanced cytotoxicity of PSO by nanodevices on the U251 cell. IC50 values measured for free PSO or HA/PSO/C NPs on the U251 cell at 24 h (a) and 48 h (b). Cell proliferation inhibition was measured by the MTT assay. Data are shown as means ± SD ($n = 5$).

cancer cells, whereas it decreases the drug concentration in normal tissues. Taken together, the combined application of chitosan and HA can modify PSO more effectively.

## 4. Conclusion

In this study, we isolated a novel anticancer oligopeptide, PSO, from *Perilla frutescens* seeds. PSO was successfully encapsulated by HA-conjugated chitosan and showed a broad-spectrum anticancer cytotoxicity with active targeting. Efficient utilization of meal protein from *Perilla frutescens* seeds, which is the by-product after oil extraction, can provide improvement of comprehensive utilization of *Perilla*. Moreover, PSO might be worth taking on further research as an anticancer candidate.

## Abbreviations

EE: Encapsulation efficiency
HA: Hyaluronic acid
HA/PSO/C: PSO-loaded hyaluronic acid-conjugated chitosan
HCl: Hydrochloric acid
HPLC: High-performance liquid chromatography

LE: Drug loading efficiency
NPs: Nanoparticles
OD: Optical density
PBS: Phosphate-buffered saline
PSO: *Perilla* seed oligopeptide
RP-HPLC: Reversed-phase high-performance liquid chromatography.

## Data Availability

The data used to support the findings of this study are available from the corresponding author upon request.

## Conflicts of Interest

No conflict of interest was declared by all authors.

## Acknowledgments

This study was supported by a grant from the National Natural Science Foundation of China (no. 51603195) and a grant from the Science and Technology Research Program in Social Development of Shanxi Province (no. 201603D321031).

## References

[1] M. Nitta, J. K. Lee, and O. Ohnishi, "Asian perilla crops and their weedy forms: their cultivation, utilization and genetic relationships," *Economic Botany*, vol. 57, no. 2, pp. 245–253, 2003.

[2] T. Zhang, C. Song, L. Song et al., "RNA sequencing and coexpression analysis reveal key genes involved in $\alpha$-linolenic acid biosynthesis in *Perilla frutescens* seed," *International Journal of Molecular Sciences*, vol. 18, no. 11, 2017.

[3] M. Asif, "Health effects of omega-3, 6, 9 fatty acids: *Perilla frutescens* is a good example of plant oils," *Oriental Pharmacy and Experimental Medicine*, vol. 11, no. 1, pp. 51–59, 2011.

[4] G. Zhao, C. Yao-Yue, G. W. Qin, and L. H. Guo, "Luteolin from purple Perilla mitigates ROS insult particularly in primary neurons," *Neurobiology of Aging*, vol. 33, no. 1, pp. 176–186, 2012.

[5] A. Y. Lee, B. R. Hwang, M. H. Lee, S. Lee, and E. J. Cho, "*Perilla frutescens* var. *japonica* and rosmarinic acid improve amyloid-$\beta_{25\text{-}35}$ induced impairment of cognition and memory function," *Nutrition Research and Practice*, vol. 10, no. 3, pp. 274–281, 2016.

[6] J. Lee, S. Park, J. Y. Lee, Y. K. Yeo, J. S. Kim, and J. Lim, "Improved spatial learning and memory by perilla diet is correlated with immunoreactivities to neurofilament and $\alpha$-synuclein in hilus of dentate gyrus," *Proteome Science*, vol. 10, no. 1, p. 72, 2012.

[7] L. Zhang, Y. J. Peng, Y. M. Niu, H. Fan, Y. J. Gao, and M. H. Chen, "Determination the contents of lutein and $\beta$-carotene in *Perilla frutescens*," *China Food Additives*, vol. 5, pp. 121–125, 2016.

[8] T. Shimokawa, A. Moriuchi, T. Hori et al., "Effect of dietary alpha-linolenate/linoleate balance on mean survival time, incidence of stroke and blood pressure of spontaneously hypertensive rats," *Life Sciences*, vol. 43, no. 25, pp. 2067–2075, 1988.

[9] Z. Y. Xiao, J. B. Jia, L. Chen, W. Zou, and X. P. Chen, "Phase I clinical trial of continuous infusion of tyroserleutide in patients with advanced hepatocellular carcinoma," *Medical Oncology*, vol. 29, no. 3, pp. 1850–1858, 2012.

[10] J. B. Jia, W. Q. Wang, and G. Lin, "Advances of tyroserleutide and tyroservaltide as novel anti-cancer agents," *Chinese Journal of New Drugs and Clinical*, vol. 28, no. 6, pp. 401–404, 2009.

[11] X. Jin, M. Li, L. Yin, J. Zhou, Z. Zhang, and H. Lv, "Tyroservatide-TPGS-paclitaxel liposomes: tyroservatide as a targeting ligand for improving breast cancer treatment," *Nanomedicine*, vol. 13, no. 3, pp. 1105–1115, 2017.

[12] S. Alonso-Álvarez, E. Pardal, D. Sánchez-Nieto et al., "Plitidepsin: design, development, and potential place in therapy," *Drug Design, Development and Therapy*, vol. 11, pp. 253–264, 2017.

[13] D. Rawat, M. Joshi, P. Joshi, and H. Atheaya, "Marine peptides and related compounds in clinical trial," *Anti-Cancer Agents in Medicinal Chemistry*, vol. 6, no. 1, pp. 33–40, 2006.

[14] G. L. Bidwell, "Peptides for cancer therapy: a drug-development opportunity and a drug-delivery challenge," *Therapeutic Delivery*, vol. 3, no. 5, pp. 609–621, 2012.

[15] V. K. Mourya and N. N. Inamdar, "Trimethyl chitosan and its applications in drug delivery," *Journal of Materials Science. Materials in Medicine*, vol. 20, no. 5, pp. 1057–1079, 2009.

[16] V. Orian-Rousseau, "CD44, a therapeutic target for metastasising tumours," *European Journal of Cancer*, vol. 46, no. 7, pp. 1271–1277, 2010.

[17] A. K. Yadav, P. Mishra, and G. P. Agrawal, "An insight on hyaluronic acid in drug targeting and drug delivery," *Journal of Drug Targeting*, vol. 16, no. 2, pp. 91–107, 2008.

[18] Y. F. Xiao, M. M. Jie, B. S. Li et al., "Peptide-based treatment: a promising cancer therapy," *Journal of Immunology Research*, vol. 2015, Article ID 761820, 13 pages, 2015.

[19] D. Wu, Y. Gao, Y. Qi, L. Chen, Y. Ma, and Y. Li, "Peptide-based cancer therapy: opportunity and challenge," *Cancer Letters*, vol. 351, no. 1, pp. 13–22, 2014.

[20] S. Marqus, E. Pirogova, and T. J. Piva, "Evaluation of the use of therapeutic peptides for cancer treatment," *Journal of Biomedical Science*, vol. 24, no. 1, p. 21, 2017.

[21] H. Qin, Y. Ding, A. Mujeeb, Y. Zhao, and G. Nie, "Tumor microenvironment targeting and responsive peptide-based nanoformulations for improved tumor therapy," *Molecular Pharmacology*, vol. 92, no. 3, pp. 219–231, 2017.

[22] R. C. Cheung, T. B. Ng, J. H. Wong, and W. Y. Chan, "Chitosan: an update on potential biomedical and pharmaceutical applications," *Marine Drugs*, vol. 13, no. 8, pp. 5156–5186, 2015.

[23] K. Park, M. Y. Lee, K. S. Kim, and S. K. Hahn, "Target specific tumor treatment by VEGF siRNA complexed with reducible polyethyleneimine-hyaluronic acid conjugate," *Biomaterials*, vol. 31, no. 19, pp. 5258–5265, 2010.

[24] C. Surace, S. Arpicco, A. Dufaÿ-Wojcicki et al., "Lipoplexes targeting the CD44 hyaluronic acid receptor for efficient transfection of breast cancer cells," *Molecular Pharmaceutics*, vol. 6, no. 4, pp. 1062–1073, 2009.

[25] R. H. Eibl, T. Pietsch, J. Moll et al., "Expression of variant CD44 epitopes in human astrocytic brain tumors," *Journal of Neuro-Oncology*, vol. 26, no. 3, pp. 165–170, 1995.

[26] J. D. Sacks and M. V. Barbolina, "Expression and function of CD44 in epithelial ovarian carcinoma," *Biomolecules*, vol. 5, no. 4, pp. 3051–3066, 2015.

[27] V. N. Nguyen, T. Mirejovský, L. Melinová, and V. Mandys, "CD44 and its v6 spliced variant in lung carcinomas: relation to NCAM, CEA, EMA and UP1 and prognostic significance," *Neoplasma*, vol. 47, no. 6, pp. 400–408, 2000.

[28] A. Avigdor, P. Goichberg, S. Shivtiel et al., "CD44 and hyaluronic acid cooperate with SDF-1 in the trafficking of human CD34+ stem/progenitor cells to bone marrow," *Blood*, vol. 103, no. 8, pp. 2981–2989, 2004.

[29] F. Khademi, R. A. Taheri, A. Yousefi Avarvand, H. Vaez, A. A. Momtazi-Borojeni, and S. Soleimanpour, "Are chitosan natural polymers suitable as adjuvant/delivery system for anti-tuberculosis vaccines?," *Microbial Pathogenesis*, vol. 121, pp. 218–223, 2018.

[30] P. Lim Soo, J. Cho, J. Grant, E. Ho, M. Piquette-Miller, and C. Allen, "Drug release mechanism of paclitaxel from a chitosan-lipid implant system: effect of swelling, degradation and morphology," *European Journal of Pharmaceutics and Biopharmaceutics*, vol. 69, no. 1, pp. 149–157, 2008.

[31] J. A. Gomes, R. Amankwah, A. Powell-Richards, and H. S. Dua, "Sodium hyaluronate (hyaluronic acid) promotes migration of human corneal epithelial cells in vitro," *The British Journal of Ophthalmology*, vol. 88, no. 6, pp. 821–825, 2004.

[32] S. Koochekpour, G. J. Pilkington, and A. Merzak, "Hyaluronic acid/CD44H interaction induces cell detachment and stimulates migration and invasion of human glioma cells in vitro," *International Journal of Cancer*, vol. 63, no. 3, pp. 450–454, 1995.

[33] G. Mattheolabakis, L. Milane, A. Singh, and M. M. Amiji, "Hyaluronic acid targeting of CD44 for cancer therapy: from receptor biology to nanomedicine," *Journal of Drug Targeting*, vol. 23, no. 7-8, pp. 605–618, 2015.